OPEN ACCESS Freely available online

PLOS ONE

Ubiquitination Increases Parkin Activity to Promote Autophagic α-Synuclein Clearance

Irina Lonskaya, Nicole M. Desforges, Michaeline L. Hebron, Charbel E-H. Moussa*

Department of Neuroscience, Laboratory for Dementia and Parkinsonism, Georgetown University Medical Center, Washington, DC, United States of America

Abstract

Parkinson's disease (PD) is a movement disorder associated with genetic and age related causes. Although autosomal recessive early onset PD linked to parkin mutations does not exhibit α-Synuclein accumulation, while autosomal dominant and sporadic PD manifest with α-Synuclein inclusions, loss of dopaminergic substantia nigra neurons is a common denominator in PD. Here we show that decreased parkin ubiquitination and loss of parkin stability impair interaction with Beclin-1 and alter α-Synuclein degradation, leading to death of dopaminergic neurons. Tyrosine kinase inhibition increases parkin ubiquitination and interaction with Beclin-1, promoting autophagic α-Synuclein clearance and nigral neuron survival. However, loss of parkin via deletion increases α-Synuclein in the blood compared to the brain, suggesting that functional parkin prevents α-Synuclein release into the blood. These studies demonstrate that parkin ubiquitination affects its protein stability and E3 ligase activity, possibly leading to α-Synuclein sequestration and subsequent clearance.

Citation: Lonskaya I, Desforges NM, Hebron ML, Moussa CE-H (2013) Ubiquitination Increases Parkin Activity to Promote Autophagic α-Synuclein Clearance. PLoS ONE 8(12): e83914. doi:10.1371/journal.pone.0083914

Editor: Kah-Leong Lim, National University of Singapore, Singapore

Received August 26, 2013; **Accepted** November 11, 2013; **Published** December 26, 2013

Funding: These studies were supported by NIH grant NIA 30378 and Georgetown University funding to Charbel E-H Moussa. The funders had no role in the study design, data collection and analysis, decision to publish, or preparation of the manuscript.

Competing Interests: Dr. Charbel Moussa has a pending application to use nilotinib and bosutinib as a treatment for neurodegenerative diseases. The PCT application number PCT/US13/039283 was filed on May 2, 2013 and claims priority to two provisional patent applications filed on May 2, 2012 and March 1, 2013. The title is "Treating neural diseases with tyrosine kinase inhibitors." The authors also confirm that they adhere to all the PLOS ONE policies on sharing data and materials, as detailed online in the guide for authors.

* E-mail: cem46@georgetown.edu

Introduction

Parkinson's disease (PD) is predominantly sporadic, but some disease-causing mutations suggest a genetic component in the pathogenesis of this disorder. Mutations in the autosomal recessive gene *Parkin* are the most common causes (50%) of familial autosomal recessive early onset PD [1,2,3,4,5], while autosomal dominant mutations in α-*SNCA* cause late onset PD [4,5]. Familial and sporadic PD are characterized by death of dopaminergic neurons in the Substantia Nigra *pars compacta* (SN) [6,7,8]. Sporadic PD pathology includes cytosolic α-Synuclein inclusions known as Lewy bodies (LBs) [9,10,11]. However loss of parkin function (via mutations) is usually not associated with LBs [12], but some parkin-linked patients have LBs [13,14,15]. α-Synuclein impairs autophagy and leads to autophagosome accumulation [16,17] perhaps leading to neuronal death. Parkin is a cytosolic E3 ubiquitin ligase that targets specific substrates for proteasomal [18,19,20] and autophagic [21,22,23,24,25] degradation. Parkin is also inactivated in sporadic PD, and accumulation of amyloidogenic proteins alters parkin solubility and enzymatic activity [26,27,28], suggesting that loss of parkin function is due to changes in protein stability independent of disease-causing mutations. Insoluble parkin is associated with loss of tyrosine hydroxylase (TH^+) neurons in sporadic PD [24]. Thus, despite the lack of genetic link between parkin and α-Synuclein, the role of parkin is supported in both familial autosomal recessive and sporadic PD [29].

Activation of the tyrosine kinase Abelson (Abl) increases α-Synuclein accumulation in α-Synuclein models and Abl inhibition increases autophagic α-Synuclein clearance [30]. Abl activation also inhibits parkin activity, and Abl inhibition activates parkin in PD models [31]. Tyrosine kinase inhibitors (TKIs) are effective and well-tolerated treatments for chronic myelogenous leukemia (CML) [32,33]. The availability of brain penetrant TKIs, including nilotinib and bosutinib [34] and the relationship between Abl and both α-Synuclein [30] and parkin [30,31,34] provide an important link to study the effects of parkin activity on α-Synuclein clearance and TH^+ neurons. We investigated the effects of ubiquitination on parkin E3 ligase activity and its role in α-Synuclein clearance and survival of SN neurons. The current studies use pharmacological (TKIs), and genetic (lentiviral gene transfer and transgenic animal) approaches in PD models.

Materials and Methods

Stereotaxic injection

Six months old male C57BL/6 mice were stereotaxically injected with lentiviral α-Synuclein (or LacZ control) bilaterally into the SN using co-ordinates: lateral: 1.5 mm, ventral: 4.1 mm and horizontal: −3.64. The lentivirus was tittered in human M17 neuroblastoma cells according to Invitrogen protocol. Titration and lentiviral expression was verified via counting the V5 tag-positive cells as virally infected cells relative to the total number of cells in 12 well dishes (Falcon). The number of viral genomes was calculated and a total number of 1×10^4 viral particles were injected into the mouse SN in a total of 6 µl. Viral stocks were injected through a microsyringe pump controller (Micro4) using total pump (World Precision Instruments, Inc.) delivery of 2 µl at a

rate of 0.2 µl/min as previously described [35,36,37]. All animal experiments were reviewed and approved Georgetown University Animal Care and Use Committee (GUAUC). n = number of animals in each experiments. Data were analyzed as mean±SEM using Graph Pad software and ANOVA with Newman Keuls post analysis or two-tailed t-test ($P<0.05$).

Nilotinib and bosutinib treatment

Three weeks post-injection with the lentivirus, half the animals were I.P. treated daily with 10 mg/Kg nilotinib of 5 mg/kg bosutinib dissolved in DMSO and the other half received DMSO treatments (3 µl total) for an additional 3 weeks. Half of A53T transgenic mice were I.P. treated daily with TKIs and the other half with DMSO. Lower drug dose, including 1 mg/Kg and 5 mg/Kg were administered I.P. every other day for 6 weeks.

Human postmortem brain tissues

Human postmortem samples were obtained from John's Hopkins University brain bank. Patients' description, sample preparation and staining are summarized in [27]. Data were analyzed as mean±SEM, using Two-tailed t-test ($P<0.05$). All studies on postmortem human tissues were reviewed and approved by Georgetown University's institutional review board.

Western blot analysis

The nigrostriatal region was isolated from α-Synuclein expressing mice and compared with LacZ or total brain extracts from A53T mice. Tissues were homogenized in 1x Sodium Tris EDTA NP40 (STEN) lysis buffer (50 mM Sodium Tris (pH 7.6), 150 mM NaCl, 2 mM EDTA, 0.2 % NP-40, 0.2 % BSA, 20 mM PMSF and protease cocktail inhibitor), centrifuged at 10,000 x g for 20 min at 4°C and the supernatant containing the soluble protein fraction was collected. The supernatant was analyzed by WB on SDS NuPAGE Bis-Tris gel (Invitrogen). Human α-Synuclein was probed (1:1500) with human antibodies (ThermoScientific). β-actin was probed (1:1000) with polyclonal antibody (Cell Signaling Technology, Beverly, MA, USA). Rabbit polyclonal Beclin-1 was used (1:1000) according to autophagy antibody sampler kit 4445 (Cell Signaling, Inc) and a rabbit polyclonal (Pierce) anti-LC3 (1:1000) were used. WBs were quantified by densitometry using Quantity One 4.6.3 software (Bio Rad).

IHC of brain sections

Animals were deeply anesthetized with a mixture of Xylazine and Ketamine (1:8), washed with 1X saline for 1 min and then perfused with 4% paraformaldehyde (PFA) for 15−20 min. Brains were quickly dissected out and immediately stored in 4% PFA for 24h at 4°C, and then transferred to 30% sucrose at 4°C for 48h. TH was probed (1:100) with rabbit polyclonal (AB152) antibody (Millipore) and human α-Synuclein was probed (1:100) with mouse monoclonal antibodies (Thermo Scientific) and DAB counterstained.

Stereological methods were applied by a blinded investigator using unbiased stereology analysis (Stereologer, Systems Planning and Analysis, Chester, MD) to determine the total positive cell counts in 20 cortical fields on at least 10 brain sections (~400 positive cells per animal) from each animal as previously explained [38].

Cell culture and transfection

B35 rat neuroblastoma cells (Gift of Dr. Cathy Conant, American Tissue Culture Center) were grown in 24 well dishes (Falcon) and transfected with 3 µg parkin cDNA for 24hrs. Cells were treated with 10 µM nilotinib or 1 µM bosutinib for 24hrs or 20 µM MG132 for 6 hrs. Cells were harvested 48 hrs after transfection and centrifuged at 10,000×g for 20 min at 4°C and the supernatant was collected.

Humanα-Synuclein ELISA were performed using 50 µl (1 µg/µl) of brain lysates (in STEN buffer) detected with 50 µl primary antibody (3h) and 100 µl anti-rabbit secondary antibody (30 min) at RT. α-Synuclein levels were measured using human specific ELISA (Invitrogen) according to manufacturers' protocols.

ELISA Dopamine and HVA

Total brain or mesencephalon were collected and fresh 50 µl (1 µg/µl) brain lysates (in STEN buffer) were detected with 50 µl primary antibody (1h) and 100 µl anti-rabbit secondary antibody (30 min) at RT according to manufacturer's protocols (Abnova, Cat# BOLD01090J00011) for DA and (Eagle Biosciences, Cat# HVA34-K01) for HVA.

Subcellular fractionation to isolate AVs- 0.5 g of fresh animal brains were homogenized at low speed (Cole-Palmer homogenizer, LabGen 7, 115 Vac) in 1xSTEN buffer and centrifuged at 1,000 g for 10 minutes to isolate the supernatant from the pellet. The pellet was re-suspended in 1xSTEN buffer and centrifuged once to increase the recovery of lysosomes. The pooled supernatants were then centrifuged at 100,000 rpm for 1 hr at 4°C to extract the pellet containing AVs and lysosomes. The pellet was then re-suspended in 10 ml (0 .33 g/ml) 50% Metrizamide and 10 ml in cellulose nitrate tubes. A discontinuous Metrizamide gradient was constructed in layers from bottom to top as follows: 6 ml of pellet suspension, 10 ml of 26%; 5 ml of 24%; 5 ml of 20%; and 5 ml of 10% Metrizamide. After centrifugation at 10,000 rpm for 1 hour at 4°C, the fraction floating on the 10% layer (Lysosome) and the fractions banding at the 24%/20% (AV 20) and the 20%/10% (AV10) Metrizamide inter-phases were collected by a syringe and examined by ELISA.

qRT-PCR in brain tissues

qRT-PCR was performed on Real-time OCR system (Applied Biosystems) with Fast SYBR-Green PCR master Mix (Applied Biosystems) in triplicate from reverse transcribed cDNA from mouse mesencephalon injected with lentiviral LacZ or lentiviral α-Synuclein (total 6 weeks) treated with DMSO or TKIs (total 3 weeks). Human wild-type α-Synuclein -CAC CAT GGA TGT ATT CAT GTT TCC- was used as a forward primer and -GGC TTC AGG TTC GTA GTC TTG AT- as a reverse primer. Gene expression values were normalized using GADPH levels.

Proximity Ligation Assay (PLA)

Primary 1:100 mouse anti-parkin (PRK8, above) and rabbit 1:100 anti-Beclin-1 (above), or ubiquitin (Life Sensors) antibodies were applied to 20 µm thick sections of mouse brain or deparrafanized PPE human brains overnight at 4°C. Duolink In Situ Red Starter Kit (Cat#92101-KI01) containing species-specific secondary antibodies or PLA probes, each with a unique short DNA strand attached to it (Axxora, LLC, Farmingdale, NW) was used as described in manufacturer's protocol. When the PLA probes are in close proximity, the DNA strands interact through a subsequent addition of two other circle-forming DNA oligonucleotides. After joining of the two added oligonucleotides by enzymatic ligation, they are amplified via rolling circle amplification using a polymerase to highlight the interaction. Fluorescence in each single-molecule amplification product is easily visible as a distinct bright spot when viewed with a fluorescence microscope.

Immunoprecipitation

Mouse brains tissues were homogenized in 1XSTEN buffer and the soluble fraction was isolated as indicated above. The lysates were pre-cleaned with immobilized recombinant protein G agarose (Pierce #20365), and centrifuged at 2500xg for 3 min at 4°C. The supernatant was recovered, and quantified by protein assay and a total of 100 mg protein was incubated for 1 hr at 4°C with primary 1:100 mouse anti-parkin (PRK8, above) and rabbit 1:100 anti-ubiquitin (Life Sensors) antibodies in the presence of sepharose G and an IgG control with primary antibodies. The immunoprecipiates were collected by centrifugation at 2500 xg for 3 min at 4°C, washed 5x in PBS, with spins of 3 min, 2500xg using detergent-free buffer for the last washing step and the proteins were eluted according to Pierce instructions (Pierce #20365). After IP, the samples were size-fractionated on 4−12% SDS-NuPAGE and transferred onto 20 µm nitrocellulose membranes. The primary antibodies used for WB analysis of the parkin and ubiquitin were the same as those used for IP. WB detection of the parkin and ubiquitin was then performed using either HRP conjugated secondary antibodies.

Immunoprecipitation and ubiquitination assay

Parkin or ubiquitin were separately immunoprecipitated in 100 µl (100 µg of proteins) 1×STEN buffer using (1:100) anti-ubiquitin monoclonal antibody (Abnova) or (1:100) anti-parkin mouse monoclonal antibody (PRK8), respectively. Following immunoprecipitation, 300 ng of each substrate protein (parkin and ubiquitin) were mixed in the presence of 1 µg recombinant human ubiquitin (Boston Biochem, MA), 100 mM ATP, 1 µg recombinant UbcH7 (Boston Biochem), 40 ng E1 recombinant enzyme (Boston Biochem) and incubated at 37°C in an incubator for 20min. The reaction was heat inactivated by boiling for 5 min and the substrates were analyzed by WB.

Parkin E3 ubiquitin ligase activity

To determine the activity of parkin E3 ligase activity. E3LITE Customizable Ubiquitin Ligase Kit (Life Sensors, UC#101), which measures the mechanisms of E1-E2-E3 activity in the presence of different ubiquitin chains was used. UbcH7 was used as an E2 that provides maximum activity with parkin E3 ligase and added E1 and E2 in the presence of recombinant ubiquitin, including WT or no Lys mutant (K0) as control. E3 was added as IP parkin to an ELISA microplate that captures poly-ubiquitin chains formed in the E3-dependent reaction, which was initiated with ATP at RT for 60 minutes. Controls included, E1-E2-E3 and assay buffer for background reading. The plates were washed 3 times and incubated with streptavidin-HRP for 5 minutes and were read on a chemiluminecense plate reader.

Results

Parkin interaction with Beclin-1 is decreased in sporadic PD brains

We previously demonstrated accumulation of insoluble parkin within autophagic vacuoles (AVs) in post-mortem sporadic PD brains [24], suggesting that decreased parkin solubility leads to autophagic defects. Immunostaining shows parkin expression in DAPI stained neurons (Fig. 1A, inset) with astrocytic glial fibrillary acidic protein (GFAP) staining and TH^+ neurons counterstained with DAB (Fig. 1B) in serial midbrain sections of healthy human subjects (See subjects' description in [24]). *In situ* proximity ligation assay (PLA) shows human parkin-Beclin-1 interaction in control midbrain neurons (Fig. 1C, n = 7), suggesting that parkin collaborate with this key autophagy enzyme. However, staining in PD midbrain shows some activated astrocytes and parkin accumulation in the cytosol of DAPI stained nuclei (Fig. 1D, inset), consistent with decreased parkin solubility in PD brains [24]. Loss of TH^+ neurons (Fig. 1E) was associated with altered parkin expression and decreased parkin-Beclin-1 interaction (Fig. 1F, n = 9). These data are consistent with our previous results showing parkin immunoprecipitation with Beclin-1 [39]. Parkin-Beclin-1 interaction was also demonstrated via parkin (Fig. 1G) and Beclin-1 (Fig. 1H) co-labeling, which showed co-localization of these two proteins in human control brains (Fig. 1I, n = 7). However, alteration of parkin expression (Fig. 1J) was observed with Beclin-1 staining (Fig. 1K) and reduced co-localization in sporadic PD brains (Fig. 1L, n = 9). Stereological counting of positive cells that show red fluorescence with PLA was significantly decreased (64%, $P<0.001$) in post-mortem PD brains (Fig. 1C, n = 9) compared to aged-matched controls (Fig. 1F, n = 7). To ascertain that this decrease in fluorescence was due to parkin-Beclin-1 interaction, post-mortem PD striatal extracts, which show significantly increased beclin-1 levels (Fig. 1N, 32%, $p<0.05$, 1st blot) relative to tubulin (2nd blot), were immunoprecipitated with Beclin-1 antibody and showed decreased levels of parkin (Fig. 1N, 3rd blot). Conversely, less Beclin-1 was detected when parkin was immunoprecipitated (Fig, 1N, 4th blot), suggesting decreased Parkin-beclin-1 interaction in agreement with our previous data [39].

TKI increases parkin ubiquitination and interaction with Beclin-1

We sought to determine whether TKIs affect parkin ubiquitination, perhaps leading to its activation and facilitated interaction with Beclin-1. PLA shows parkin-Beclin-1 interaction in the striatum of wild type (WT) C57BL/6 (Fig. 2A, n = 5) but not $parkin^{-/-}$ mice generated on the same background [40] (Fig. 2B, n = 5). We previously showed that nilotinib decreases α-Synuclein level in a mouse model that harbors human mutant A53T α-Synuclein under the mouse prion protein promoter [30,41]. Parkin-Beclin-1 interaction in the striatum was decreased (84% by stereology) in 6 months old transgenic A53T mice treated with daily intraperotineal (I.P) injection of 30 µL DMSO for 3 weeks (Fig. 2C, n = 5), but 10 mg/kg nilotinib (Fig. 2D) or 5 mg/kg bosutinib (Fig. 2E) reversed loss of parkin-Beclin-1 interaction (63% and 81% back to control, respectively), suggesting that TKI may affect parkin activity. To determine whether TKIs affect parkin ubiquitination, PLA was performed and showed parkin-ubiquitin interaction in WT mice (Fig. 2F) but not $parkin^{-/-}$ (data not shown). Parkin-ubiquitin interaction was difficult to detect in A53T mice (Fig. 2G) treated with DMSO, but nilotinib (Fig. 2H) significantly increased parkin-ubiquitin signaling (28%) relative to control, and bosutinib (Fig. 2I) restored this signal back to control levels (n = 5), suggesting increased parkin ubiquitination. To ascertain that TKI increases parkin ubiquitination, B35 rat neuroblastoma cells (Gift of Dr. Cathy Conant) were transfected with 3 µg parkin cDNA and treated with either 10 µM nilotinib or 1 µM bosutinib for 24 hrs after transfection and the proteasome was inhibited with 20 µM MG132 for 6 hrs. To determine parkin ubiquitination, parkin (E3) was immuno-precipitated and E1, E2 (UbcH7) enzymes were added with ATP and either WT or K0 ubiquitin as we previously described [38]. Parkin ubiquitination was observed with WT ubiquitin not the K0 control (Fig. 2J, n = 6), compared to recombinant E1-E2-E3 control. Nilotinib (24 hrs) significantly increased parkin poly-ubiquitination compared to DMSO (Fig. 2J, 160%, n = 6, $p<0.001$), but MG132 significantly increased parkin ubiquitination (230%, $p<0.001$). Similarly, bosutinib (24hrs) significantly increased parkin ubiquitination compared to DMSO (68%, n = 6, $p<0.001$) and MG132 further

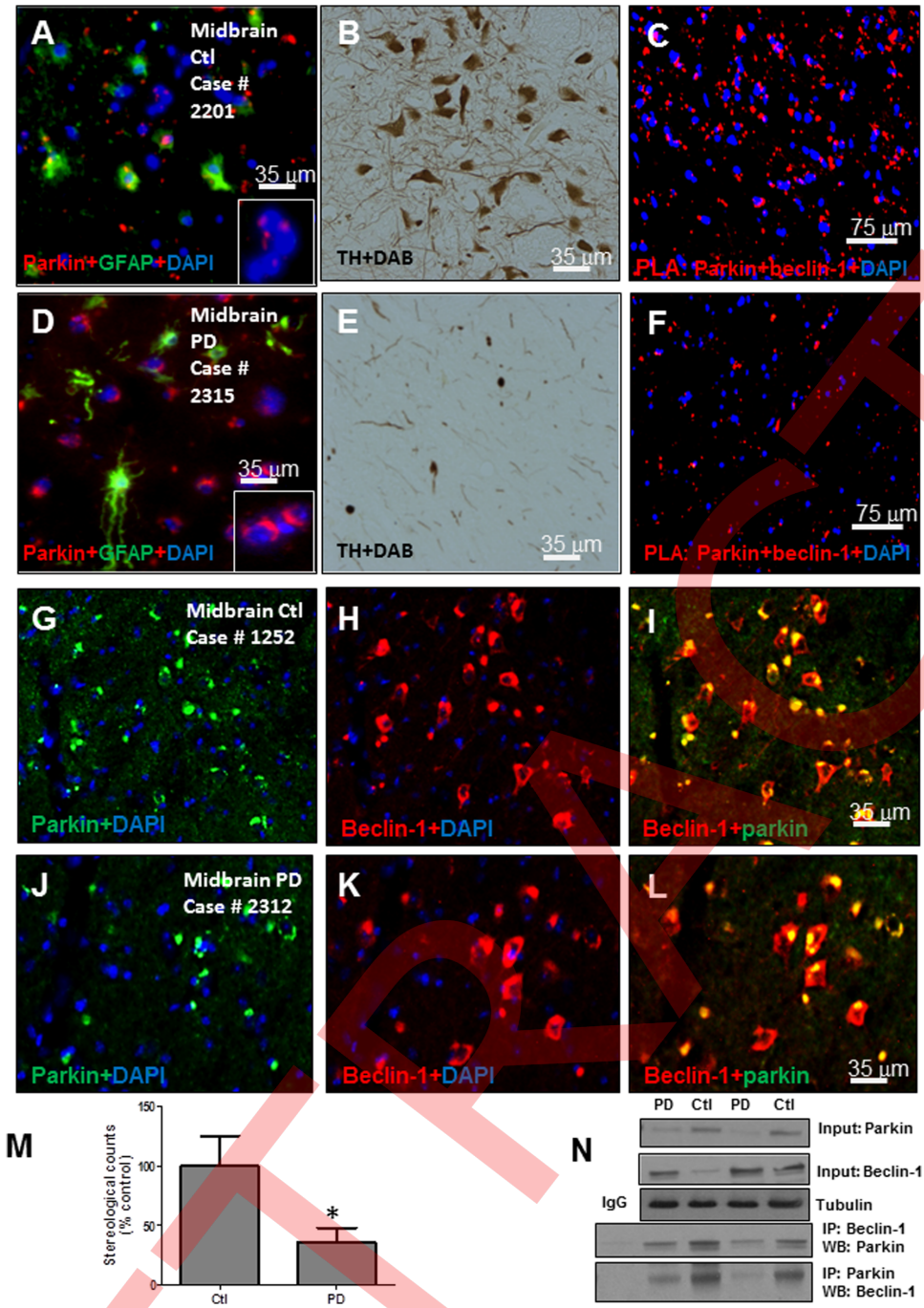

Figure 1. **Parkin co-localizes with Beclin-1 in human brain but their interaction is decreased in sporadic PD**. Immunostaining of paraffin embedded 20 µm thick human midbrain sections **A**) shows parkin expression in DAPI stained neurons co-labeled with GFAP. Inset is higher magnification showing parkin expression. **B**) TH^+ neurons counterstained with DAB in serial midbrain sections of healthy human subjects. **C**) *In situ* proximity ligation assay (PLA) shows human parkin-Beclin-1 interaction in control midbrain neurons (n = 7). **D**) Parkin expression in DAPI stained neurons co-labeled with GFAP indicating active astrocytes. Inset is higher magnification showing cytosolic parkin accumulation. **E**) TH^+ neurons counterstained with DAB in serial midbrain sections of post-mortem PD brains. **F)** *In situ* PLA shows reduced human parkin-Beclin-1 interaction in midbrain neurons in PD brains (n = 9). **G**). parkin and **H**) and Beclin-1 labeling are co-localized **I**) in human midbrain sections (n = 7). **J**) shows alteration of parkin expression and **K**) Beclin-1 staining with **L**) reduced co-localization in sporadic PD brains (n = 9). **M**) graph represents stereological counting of C and F *in situ* PLA and **N**) WB analysis on 4−12% NuPage SDS gel showing beclin-1 levels relative to actin and immunoprecipitation in post-mortem human brain tissues. Asterisk indicates significantly different, means±SEM, ANOVA, Newman Keuls. Fig 1F appears similar to material previously published in https://doi.org/10.1002/emmm.201302771 under a CC BY 3.0 Unported Deed license.
doi:10.1371/journal.pone.0083914.g001

increased parkin ubiquitination (150%, $p<0.0001$), suggesting that TKI increases ubiquitinated parkin, which is degraded via the proteasome. Parkin was immunoprecipitated from transfected B35 cells and *in-vitro* ubiquitination assay was also performed as we previously described [35,38]. Higher levels of ubiquitinated parkin were observed in nilotinib and bosutinib treated cells compared to DMSO (Fig. 2K, $n = 5$), suggesting an increase in parkin ubiquitination. However, MG132 further increased the protein smear with TKIs, indicating that ubiquitinated parkin is quickly degraded via the proteasome.

TKIs increase parkin level and stimulate autophagic α-Synuclein clearance in A53T mice

To test the effects of prolonged TKI using lower drug dose, 1 month old A53T mice were injected I.P. with either 5 mg/kg or 1 mg/kg bosutinib once every other day for 6 weeks and α-Synuclein was measured by enzyme-linked immunosorbent assay (ELISA). Human α-Synuclein was significantly decreased from 830 ng/ml in DMSO treated mice to 580 ng/ml (5 mg/kg) and 606 ng/ml (1 mg/kg) in brain lysates (Fig. 3A, $p<0.001$, $n = 10$). The whole blood was collected via cardiac puncture and extracted in the same STEN lysis buffer used for brain lysates and analyzed by ELISA. Human α-Synuclein was also detected in the blood of DMSO-treated A53T mice (Fig. 3B, 1635 ng/ml, $p<0.0001$, $n = 10$), but 5 mg/kg and 1 mg/kg bosutinib significantly decreased α-Synuclein levels (1305 ng/ml and 1093 ng/ml, respectively, $p<0.001$). We previously showed that nilotinib clears α-Synuclein via autophagy in cell culture (using Bafilomycin A as control) and animal models *in vivo* using subcellular fractionation [30]. Subcellular fractionation of total brain lysates from A53T mice resulted in separation of AVs into AV10 and AV20, which are indicative of autophagosomes due to light chain protein-3 (LC3)-B detection (Fig. 3C, inset) and lysosomal fractions containing lysosome-associated membrane protein (LAMP2a). We also probed for a cytosolic protein marker, tubulin, which was also detectable in the extracts. Age dependent studies (Fig. 3C) show accumulation of human α-Synuclein (ELISA) in AV10 (340 ng/ml) and AV20 (401 ng/ml) in 1 month old A53T brains, but daily I.P. injection with 10 mg/kg nilotinib for 3 weeks significantly decreased α-Synuclein in AV10 (50 ng/ml, $p<0.00001$, $n = 5$) and increased it in the lysosome (268 ng/ml) compared to DMSO. Similarly, daily I.P. injection with 5 mg/kg bosutinib for 3 weeks significantly decreased α-Synuclein in AV10 (42 ng/ml, $p<0.00001$, $n = 5$) and increased it in the lysosomes (301 ng/ml) compared to DMSO. Significantly higher levels of α-Synuclein were detected in AV10 (940 ng/ml) in DMSO-treated 5 months old A53T mice (Fig. 3C, $p<0.00001$, $n = 5$) compared to 1 month old animals, but nilotinib significantly decreased α-Synuclein levels in AV10 (245 ng/ml, $n = 5$) and increased in AV20 (642 ng/ml compared to 410 ng/ml DMSO) and lysosomes (333 ng/ml), indicating increased autophagic flux *in vivo*. Similarly, bosutinib significantly decreased α-Synuclein levels in AV10 (301 ng/ml, $n = 5$) and increased in AV20 (569 ng/ml) and lysosomes (378 ng/ml).

ELISA measurement showed a slight decrease in parkin (Fig. 3D, 16%, $n = 10$) in total A53T mice brain lysates compared to WT animals and parkin$^{-/-}$, but parkin level was significantly increased ($p<0.05$) following nilotinib (24%) and bosutinib (19%) treatment compared to DMSO. We previously demonstrated autophagic parkin degradation in post-mortem PD brains [24], suggesting that failure of proteasomal degradation of insoluble parkin stimulates parkin clearance via autophagy. Parkin was not detected in AVs in WT mice with and without TKI (Fig. 3E, $n = 5$), but 1 month old A53T mice had 145 ng/ml in AV10 and 126 ng/ml in AV20, indicating parkin accumulation in autophagosome, in agreement with human data [24]. Interestingly, nilotinib and bosutinib significantly decreased parkin levels in AV20 (74 ng/ml and 68 ng/ml, respectively) not AV10, and increased it in the lysosomes (41 ng/ml and 63 ng/ml, respectively) compared to DMSO-treated A53T mice ($p<0.0001$, $n = 5$). Parkin levels were significantly increased (Fig. 3E, $p<0.002$, $n = 5$) in the brain of 5 months old A53T mice (DMSO) in AV10 (196 ng/ml), AV20 (161 ng/ml) and lysosomes (35 ng/ml) compared to 1 month old A53T mice treated with DMSO, indicating further accumulation of parkin with aging. Parkin levels were not significantly changed in AV10 but both nilotinib and bosutinib decreased parkin in AV20 (76 ng/ml and 75 ng/ml, respectively) and increased it in the lysosomes (81 ng/ml and 102 ng/ml, respectively) compared to DMSO (Fig. 3E, $p<0.003$, $n = 5$). The shift in the contents of AVs suggests that TKI increases autophagic flux to degrade accumulating misfolded proteins.

We further determined the effects of bosutinib on endogenous α-Synuclein clearance, using mouse antibodies. The endogenous levels of parkin were not affected in 7–8-month-old A53T mice compared to control (Fig. 3F, 1st), but daily i.p. injection of 5 mg/kg bosutinib for 3 weeks slightly increased parkin level (Fig. 3F, 2nd blot) and decreased monomeric (53%) and high molecular weight human α-Synuclein (Fig. 3F, $p<0.05$, $n = 9$) relative to actin compared with A53T mice treated with DMSO. These data are consistent with our previous results showing the effects of nilotinib on α-Synuclein clearance in A53T mice [30].

TKI clears α-Synuclein and protects TH$^+$ neurons in a parkin-dependent manner

To determine the effects of parkin activity on TH$^+$ neurons, 6 months old male WT and parkin$^{-/-}$ mice were stereotaxically injected with 1×10^4 m.o.i lentiviral human WT α-Synuclein (or LacZ) bilaterally into the SN for 3 weeks, and then half were treated daily with I.P. injection of 10 mg/kg nilotinib or 5 mg/kg bosutinib and the other half with DMSO (30 µl) for 3 additional weeks. Staining of 20 µm thick brain sections showed expression of human α-Synuclein in mice injected with lentiviral α-Synuclein into the SN and treated with DMSO (Fig. 4C) compared to LacZ injected WT mice treated with DMSO (Fig. 4A, $n = 10$) or bosutinib (Fig. 4B, $n = 10$); but bosutinib led to 76% (Fig. 4U, by stereology) decrease of humanα-Synuclein (Fig. 4D, $p<0.001$, $n = 10$) in SN neurons, consistent with our previously published effects with nilotinib [30]. A significant decrease in TH$^+$ neurons (Fig. 4U, 91% by stereology, $p<0.002$, $n = 10$) was observed in lentiviral α-Synuclein treated with DMSO (Fig. 4G) compared to LacZ treated with DMSO (Fig. 4E) and bosutinib (Fig. 4F), but bosutinib treatment of α-Synuclein expressing mice reversed TH$^+$ neuron loss back to 74% (Fig. 4H&U, by stereology) of DMSO level ($p<0.003$, $n = 10$). Human α-Synuclein expression in the SN of parkin$^{-/-}$ mice (Fig. 4J, $n = 10$) treated with DMSO was detected compared to LacZ injected mice (Fig. 4I), but α-Synuclein expression was unchanged in SN of parkin$^{-/-}$ mice with either bosutinib (Fig. 4K) or nilotinib (Fig. 4L) treatment ($n = 10$), suggesting that parkin is required to clear α-Synuclein. The level of TH$^+$ neurons in the SN of LacZ-injected parkin$^{-/-}$ (Fig. 4M&O) was not different from WT mice (Fig. 4E), but α-Synuclein expression significantly reduced TH$^+$ neurons (Fig. 4N,R&U, $p<0.003$, 92% by stereology, $n = 10$), and bosutinib (Fig. 4O&S) and nilotinib (Fig. 4P&T) failed to reverse these effects. To ascertain that TKI effects are due to α-Synuclein clearance and not to change in α-Synuclein gene expression, and to control for equal gene expression in lentiviral-injected mice, RT-PCR was performed to show equal amount of α-Synuclein

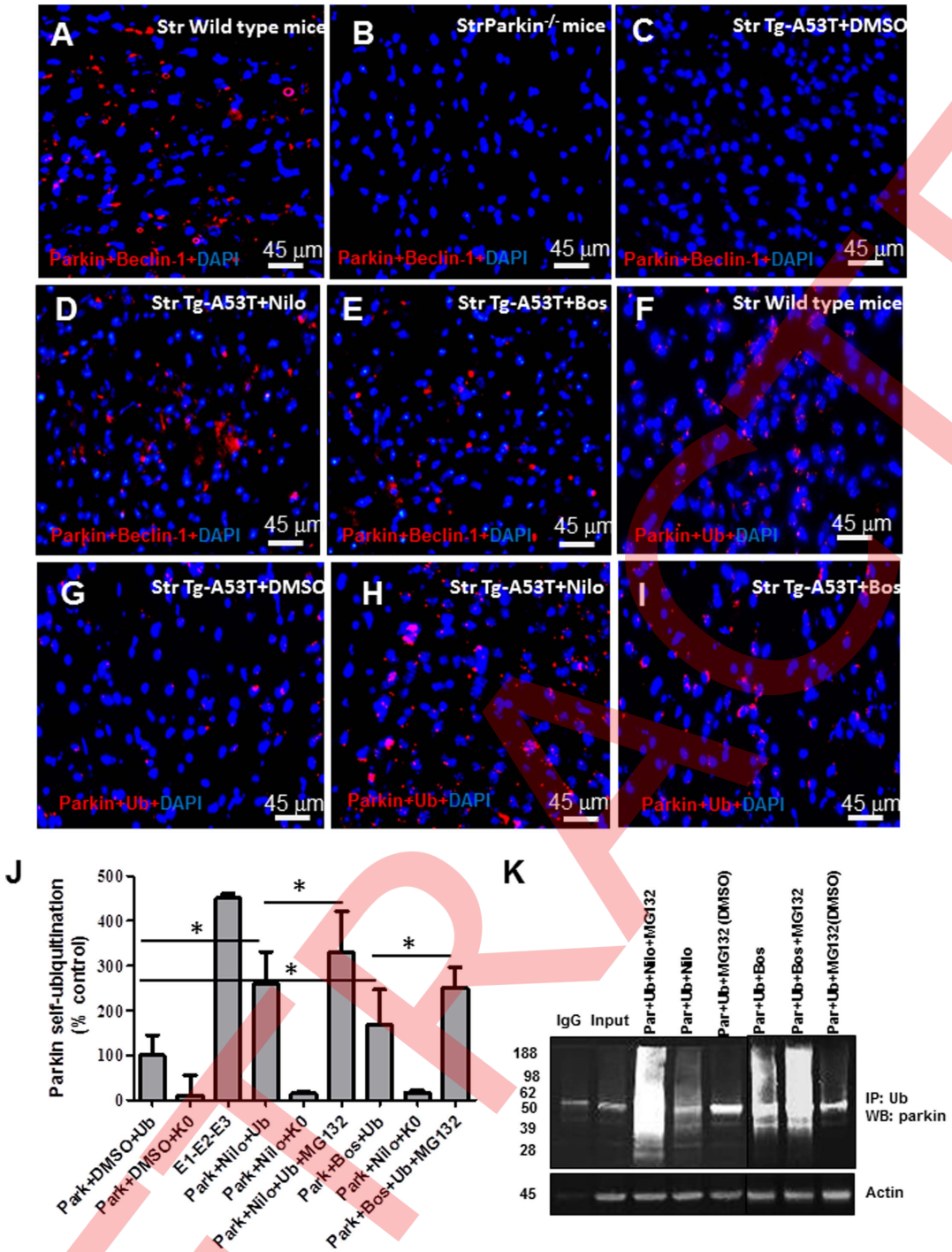

Figure 2. TKI increases parkin ubiquitination and interaction with Beclin-1. *In Situ* PLA in 20 μm thick mouse brain sections shows **A**) parkin-Beclin-1 interaction in the striatum of C57BL/6 control, **B**) parkin$^{-/-}$ mice, **C**) transgenic A53T mice treated with daily I.P injection for 3 weeks of DMSO **D**) 10 mg/kg nilotinib and **E**) 5 mg/kg bosutinib (n = 5). *In situ* PLA in 20 μm thick mouse brain sections showing parkin ubiquitination via **F**) parkin-ubiquitin interaction in the striatum of C57BL/6 control, **G**) transgenic A53T mice treated with daily I.P injection for 3 weeks of DMSO **H**) 10 mg/kg nilotinib and **I**) 5 mg/kg bosutinib (n = 5). **J**) Histograms represent parkin ubiquitination in B35 rat neuroblastoma cells treated with either 10 μM nilotinib or 1 μM bosutinib and 20 μM proteasome inhibitor MG132. Parkin ubiquitination was observed with WT ubiquitin not the K0 control (n = 6), compared to recombinant E1-E2-E3 control. Asterisk indicates significantly different, means ± SEM, ANOVA, Newman Keuls, n = 6) and **K**). immunoprecipitation of cell extracts with anti-ubiquitin antibodies and WB with parkin showing ubiquitinated proteins (n = 5).
doi:10.1371/journal.pone.0083914.g002

mRNA relative to GADPH in both parkin$^{-/-}$ and WT mice with and without TKIs (Fig. 4V, n = 10). Specific human α-Synuclein primers that were initially used in the cloning of α-Synuclein into the lentiviral plasmid were used to determine α-Synuclein mRNA levels.

Parkin deletion increases α-Synuclein secretion from the brain into the blood

To evaluate whether the decrease in blood α-Synuclein (Fig. 3B) is due to degradation of brain and/or blood α-Synuclein, which is abundantly expressed in peripheral organs of A53T mice [41], the lentiviral models that express human α-Synuclein in the brain alone were used. ELISA in SN lysates showed that human α-Synuclein levels peaked at 209 ng/ml in lentiviral α-Synuclein mice treated with DMSO, and both nilotinib and bosutinib significantly decreased α-Synuclein (45 ng/ml and 51 ng/ml, respectively) compared to DMSO (Fig. 5A, $p<0.0001$, n = 10) in WT mice. A slightly higher level of α-Synuclein (245 ng/ml) was detected in parkin$^{-/-}$ mice injected with lentiviral α-Synuclein (Fig. 4A, n = 10) compared to WT mice treated with DMSO, but nilotinib and bosutinib failed to clear α-Synuclein (206 ng/ml and 221 ng/ml, respectively) in parkin$^{-/-}$ SN lysates (Fig. 5A, $p<0.05$, n = 10) compared to DMSO treated mice. Surprisingly, human α-Synuclein was detected in the blood (Fig. 5B, 19 ng/ml, n = 10) of lentiviral α-Synuclein-injected WT mice treated with DMSO, but TKIs eliminated α-Synuclein, suggesting that brain degradation of α-Synuclein prevents its secretion into the blood. However, significantly higher levels of human α-Synuclein was detected in the blood of parkin$^{-/-}$ mice (Fig. 5B, 34 ng/ml, $p<0.04$, n = 10) compared to WT mice treated with DMSO, but neither nilotinib nor bosutinib reduced α-Synuclein (31 ng/ml), further suggesting that lack of α-Synuclein sequestration and degradation results in more α-Synuclein release from the brain into the blood.

To determine the fate of human α-Synuclein in WT and parkin$^{-/-}$ mice, ELISA was performed in AVs extracted from midbrain tissues. Human α-Synuclein was detected in AV10 (180 ng/ml) and AV20 (120 ng/ml) in lentiviral α-Synuclein expressing WT mice treated with DMSO (Fig. 5C, n = 5), but nilotinib and bosutinib significantly decreased α-Synuclein in AV10 (31 ng/ml and 49 ng/ml, respectively, $p<0.0001$, n = 5) and increased it in the lysosome (75 ng/ml and 89 ng/ml, respectively. $p<0.0001$) compared to DMSO (11 ng/ml). However, significantly less α-Synuclein was detected in AV10 (110 ng/ml, $p<0.0001$, n = 5) and AV20 (19 ng/ml) in parkin$^{-/-}$ mice expressing lentiviral α-Synuclein compared to WT with DMSO. Additionally, no differences in α-Synuclein levels in AVs were observed in nilotinib and bosutinib compared to DMSO treated parkin$^{-/-}$ mice, suggesting less α-Synuclein degradation via the autophagy-lysosome system in parkin$^{-/-}$ mice. WB analysis shows a significant increase (43%) in lentiviral α-Synuclein expressing WT and parkin$^{-/-}$ mice treated with DMSO (Fig. 5, n = 10, $p<0.05$), and appearance of higher molecular weight bands in these mice. However, nilotinib and bosutinib reversed monomeric and higher molecular weight α-Synuclein back to control levels in WT, but not parkin$^{-/-}$, mice. The level of Beclin-1 was significantly increased in parkin$^{-/-}$ mice with and without α-Synuclein expression or TKI (Fig. 5D, 85% by densitometry, $p<0.002$, n = 12) compared to WT mice. The levels of LC3-II were significantly increased relative to LC3-I (41%, $p<0.05$) and actin (120%, $p<0.002$) in parkin$^{-/-}$ mice and this did not change with TKI compared to WT mice. However, α-Synuclein increased LC3-II levels relative to LC3-I (40%, $p<0.05$) and actin (47%, $p<0.05$) in WT mice, indicating induction of autophagy, while nilotinib and bosutinib reduced LC3-II levels relative to LC3-I (61% and 43%, respectively, $p<0.04$) and actin (31% and 24%, respectively, $p<0.05$) compared to DMSO treated WT mice (Fig. 5D, n = 12). The clearance of LC3-II in WT mice treated with TKIs suggests degradation of accumulated autophagosomes, consistent with the subcellular fractionation data, whereas the lack of changes in parkin$^{-/-}$ mice indicates deficiency in the autophagosome-lysosome pathway.

ELISA quantification of dopamine and its metabolite homovanillic acid (HVA) shows significantly decreased levels of dopamine (Fig. 5E, 62%, $p<0.001$, n = 10) and HVA (36%, $p<0.03$) in α-Synuclein-expressing WT mice treated with DMSO, and nilotinib and bosutinib completely reversed dopamine and HVA back to control levels (Fig. 5E, n = 10). The level of dopamine and HVA were significantly higher in LacZ-injected parkin$^{-/-}$ mice (272% and 311%, respectively, $p<0.0001$) compared to WT treated with DMSO, suggesting that parkin may control dopamine levels [42]. However, α-Synuclein expression results in significant reduction in dopamine and HVA (110% and 54%, respectively) compared to LacZ-injected parkin$^{-/-}$ mice ($p<0.002$, n = 10) and TKIs does not affect dopamine and HVA levels in parkin$^{-/-}$ mice, consistent with the effects of these drugs on TH^{+} neurons. The increase in dopamine levels in parkin$^{-/-}$ mice compared to WT despite loss of SN neurons may be due to parkin effects on dopamine levels in the ventral tegmental area.

Discussion

These data reveal novel mechanisms pertaining to parkin protection of SN neurons. Although, parkin co-localizes with Beclin-1 in the human brain, functional interaction between these proteins is reduced [34] in post-mortem PD brains and α-Synuclein models, suggesting that aging leads to parkin inactivation independent of disease causing mutations. Importantly, increased parkin ubiquitination suggests E3 ligase activation and recycling via the proteasome, leading to maintenance of homeostatic level of functional parkin. However, loss of protein stability (insolubility) as we previously demonstrated [24], leads to parkin accumulation and degradation via autophagy, suggesting that parkin ubiquitination leads to protein stability. These data are congruent with parkin structure, which contains 9 potential ubiquitination sites on Lys residues [43], and its function as a hybrid RING (really interesting new gene) and HECT (homologous to the E6AP carboxyl terminus) enzyme [43,44,45,46,47,48], suggesting that ubiquitination may sequentially lead to parkin activation, substrate recruitment and subsequent proteasomal degradation of parkin and its substrate. Parkin is present in an auto-inhibited and inactive form usually [49] due to the complexity of its structure [43,50,51], however mutations may alter its allosteric conformation, leading to protein instability and affect enzymatic activity [43,50,51]. E3 ubiquitin ligases mediate substrate ubiquitination and may also regulate their own activity and stability via self-ubiquitination or ubiquitination by other E3 ubiquitin ligases. Here we show that parkin is auto-ubiquitinated and we previously demonstrated that parkin is auto-ubiquitinated via both Lys^{48}- and Lys^{63}-linked ubiquitin chains, leading to ubiquitination of its substrate [38]. Parkin activity is also auto-regulated through its ubiquitin-like domain, which may sterically hinder ubiquitin-conjugating E2 enzyme interaction with the catalytic center [52]. Parkin increases proteasome activity and facilitates autophagic clearance in models of neurodegeneration [24,25,35,36,37,53,54]. The increase in insoluble parkin in post-mortem sporadic PD brains [24,25] suggests that de-ubiquitination

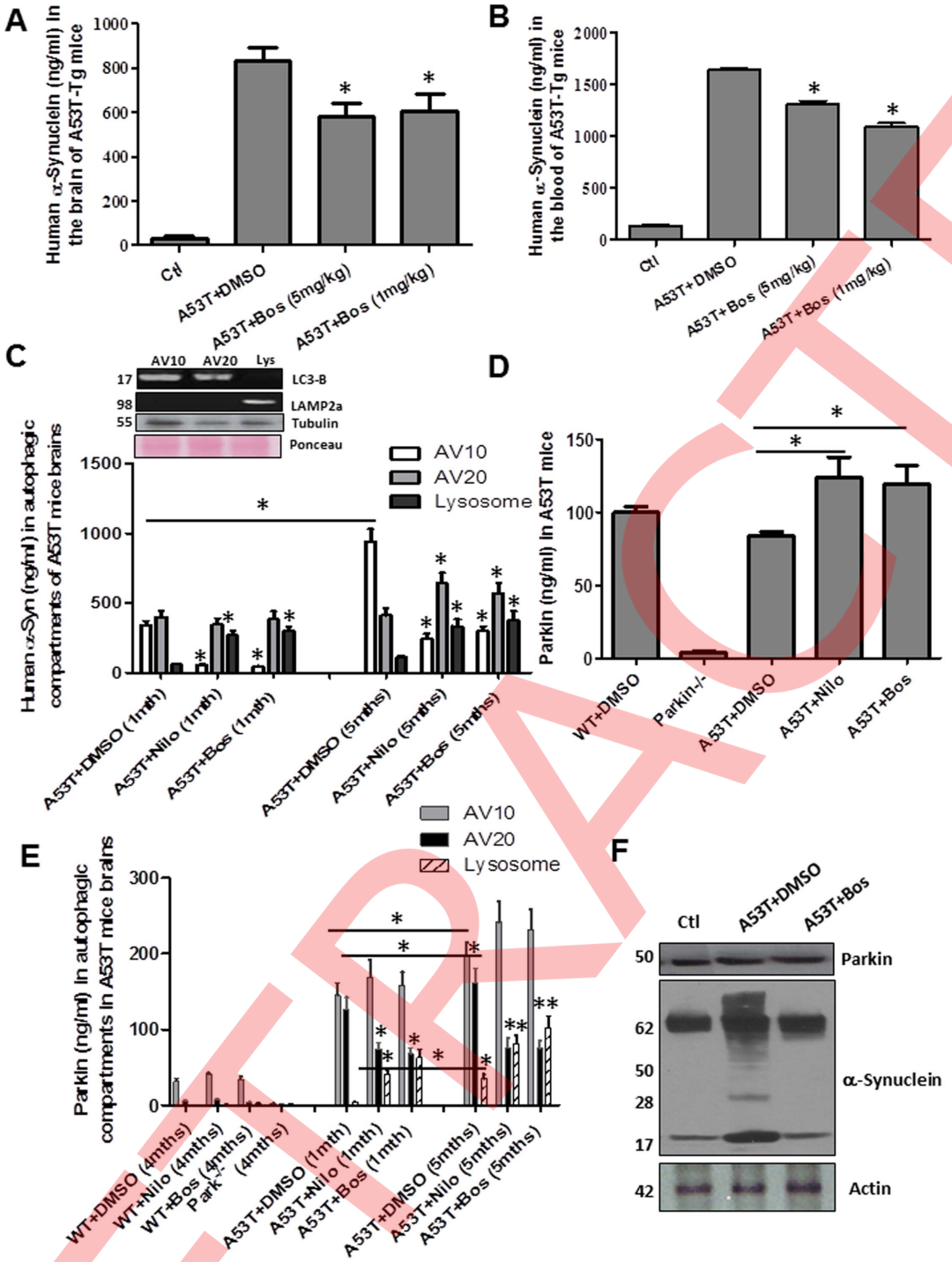

Figure 3. TKIs stimulate autophagic α-Synuclein clearance in A53T mice. ELISA measurement of human α-Synuclein in the **A**) brain and **B**) blood of 1 month old A53T mice injected I.P. with either 5 mg/kg or 1 mg/kg bosutinib once every other day for 6 weeks (n = 10). **C**). Insert shows separation of AVs and lysosomal fractions. Histograms represent subcellular fractionation of total brain lysates from A53T mice and ELISA of human α-Synuclein in AVs in 1 and 5 months old A53T brains after daily I.P. injection with 10 mg/kg nilotinib or 5 mg/kg bosutinib for 3 weeks (n = 5). **D**). ELISA showing parkin level in total brain extracts of A53T mice compared to WT and parkin$^{-/-}$ in the presence of nilotinib and bosutinib (n = 10). **E**). Histograms represent subcellular fractionation of total brain lysates from A53T mice and parkin ELISA in AVs in 1 and 5 months old A53T brains after daily I.P. injection with 10 mg/kg nilotinib or 5 mg/kg bosutinib for 3 weeks (n = 5). Asterisk indicates significantly different, means ± SEM, ANOVA, Newman Keuls. F) WB analysis on 4−12% NuPage SDS gel showing parkin and α-Synuclein levels relative to actin in A53T mice treated with either DMSO or bosutinib.

doi:10.1371/journal.pone.0083914.g003

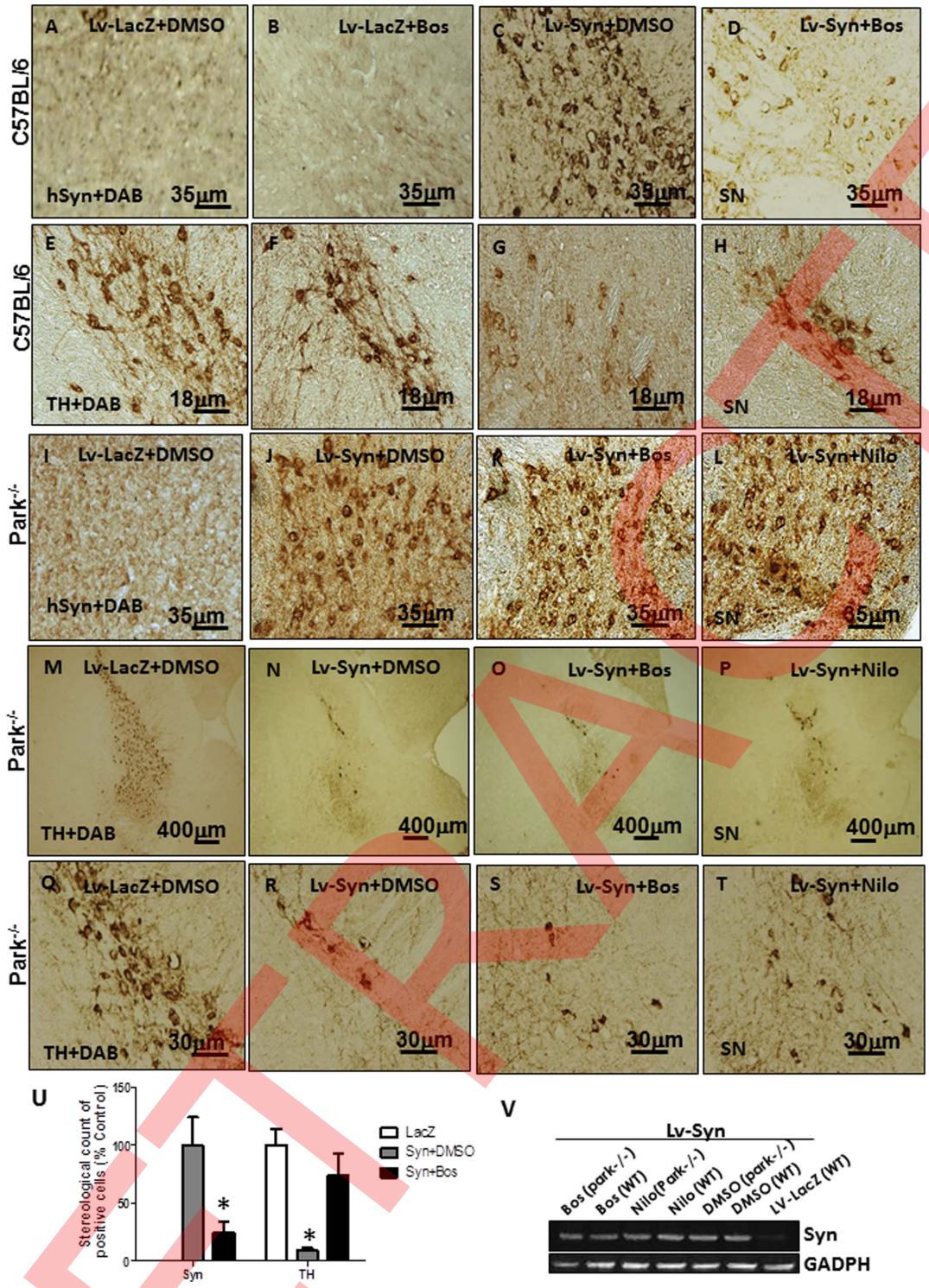

Figure 4. TKI clears α-Synuclein and protects TH$^+$ neurons in a parkin-dependent manner. Immunostaining of 20 µm thick mouse brain sections showing human α-Synuclein counterstained with DAB in the SN of lentiviral injected **A**) LacZ WT mice treated with DMSO for 3 weeks, **B**) LacZ WT treated with 5 mg/kg bosutinib, **C**) human WT α-Synuclein in WT mice treated with DMSO, and **D**) human WT α-Synuclein in WT mice treated with 5 mg/kg bosutinib (n = 10). TH$^+$ labeling counterstained with DAB in the SN of lentiviral injected **E**) LacZ WT mice treated with DMSO for 3 weeks, **F**) LacZ WT treated with 5 mg/kg bosutinib, **G**) human WT α-Synuclein in WT mice treated with DMSO, and **H**) human WT α-Synuclein in WT mice treated with 5 mg/kg bosutinib (n = 10). Human α-Synuclein in the SN of parkin$^{-/-}$ mice counterstained with DAB injected with **I)** LacZ treated with DMSO, or human α-Synuclein treated with **J**) DMSO, **K**) 5 mg/kg bosutinib and **L**) 10 mg/kg nilotinib for 3 weeks (n = 10). Staining of TH$^+$ neurons in the SN of parkin$^{-/-}$ mice counterstained with DAB injected with **M**) LacZ treated with DMSO **O**) is higher magnification, or lentiviral α-Synuclein treated with **N**) DMSO, **R**) is a higher magnification **O**) 5 mg/kg bosutinib, **S**) is a higher magnification and **P**) 10 mg/kg nilotinib, **T**) is a higher magnification (n = 10). **U**) graph represents stereological counting and **V**) RT-PCR showing equal amount of α-Synuclein mRNA relative to GADPH in both parkin$^{-/-}$ and WT mice with and without TKIs (n = 10). Asterisk indicates significantly different, means±SEM, ANOVA, Newman Keuls. Figs 4J, 4K, and 4L are excluded from this article's CC BY license. See the accompanying retraction notice for more information.
doi:10.1371/journal.pone.0083914.g004

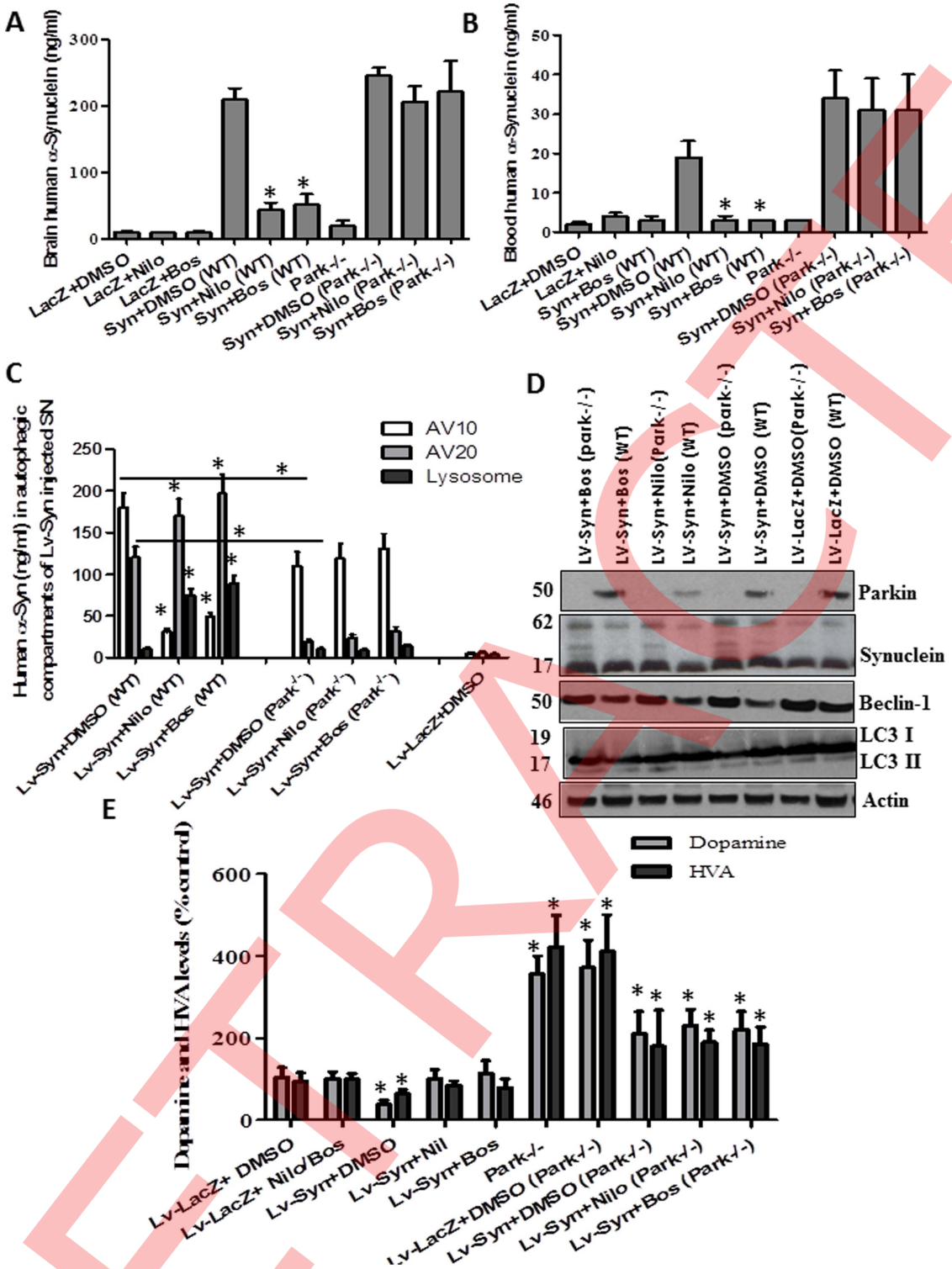

Figure 5. Parkin deletion increases α-Synuclein secretion from the brain into the blood. Histograms represent ELISA in WT and parkin$^{-/-}$ mice stereotaxically injected with lentiviral human α-Synuclein or LacZ showing α-Synuclein levels in **A**) brain lysates and **B**) total blood (n = 10) in mice treated with DMSO, 10 mg/kg nilotinib or 5 mg/kg bosutinib for 3 weeks. **C**). Histograms represent subcellular fractionation of midbrain lysates and ELISA of human α-Synuclein in AVs of WT and parkin$^{-/-}$ mice after daily I.P. injection with DMSO, 10 mg/kg nilotinib or 5 mg/kg bosutinib for 3 weeks (n = 5). **D**) WB on 4−12% SDS-NuPAGE gel showing parkin (1st blot), α-Synuclein (2nd blot) Beclin-1 (3rd blot) and LC3-I/LC3-II (4th blot) relative to actin (5th blot). **E**). Histograms represent dopamine and HVA levels in total brain lysates in WT and parkin$^{-/-}$ mice injected with lentiviral α-Synuclein or LacZ and treated with daily I.P. of DMSO, 10 mg/kg nilotinib or 5 mg/kg bosutinib for 3 weeks (n = 10). Asterisk indicates significantly different, means±SEM, ANOVA, Newman Keuls, $p<0.05$.

doi:10.1371/journal.pone.0083914.g005

may decrease parkin solubility/stability, leading to its clearance via autophagy. However, bosutinib and nilotinib increase parkin ubiquitination; facilitating its dual role in proteasomal activity as well as autophagic degradation via increased parkin-Beclin-1 interaction.

A role for parkin was described in sporadic amyotrophic lateral sclerosis (ALS) and frontotemporal lobar dementia (FTLD) [55] and in cases of mutations in valosin-containing protein (VCP) causing multisystem degeneration [56]. Parkin solubility is also altered in ALS/FTLD animal models [38] and post-mortem Alzheimer's disease (AD) brains [27]. Thus, loss of parkin E3 ubiquitin ligase function could cause neurodegeneration independent of familial PD-linked mutations in several human diseases. Although some PD-linked *Parkin* mutations induce loss of parkin function either via catalytic impairment or decreased parkin solubility and stability [57,58], other mutations have no impact on parkin activity or solubility and no known pathological consequences [59]. Our data show that TKI increases parkin ubiquitination, promoting autophagic α-Synuclein degradation and protection of SN neurons. These results are in agreement with our previous results that exogenous parkin expression or nilotinib can lead to α-Synuclein clearance [24,30]. Moreover, α-Synuclein detection in the blood of gene transfer animals is a novel finding, indicating that α-Synuclein can be released from the brain. Taken together, these data suggest that parkin-linked PD cases may have no LB inclusions due to failure of α-Synuclein sequestration en route to autophagic degradation. Although cerebrospinal fluid (CSF) α-Synuclein is thought to be derived from the brain in sporadic PD [60], it is unknown whether there is a difference in the level of α-Synuclein in the blood or CSF between parkin-linked mutations and sporadic PD. Parkin inactivation due to decreased solubility and reduced enzymatic activity [26,27,28] may result in α-Synuclein accumulation and LB formation over time in sporadic PD. Nonetheless, the common loss of SN neurons in both parkin-linked mutations and sporadic PD may be due to perturbation of dopamine levels [42,61], independent of LB formation.

In conclusion, a decrease in parkin ubiquitination may lead to protein instability and E3 ligase inactivation, causing impairment of proteasomal recycling and reduced interaction with autophagy enzymes, including Beclin-1. However, the FDA-approved CML drugs, nilotinib and bosutinib, increase parkin ubiquitination and enhance its ligase function in proteasomal and autophagic clearance. These studies provide novel mechanistic insights into PD pathology and offer strong translational promises in the therapeutic quest for PD. Parkin may be activated as a therapeutic target in neurodegenerative diseases.

Author Contributions

Conceived and designed the experiments: CM. Performed the experiments: CM IL ND MH. Analyzed the data: CM IL ND MH. Wrote the paper: CM.

References

1. Kitada T, Asakawa S, Hattori N, Matsumine H, Yamamura Y, et al. (1998) Mutations in the parkin gene cause autosomal recessive juvenile parkinsonism. Nature 392: 605–608.
2. Hattori N, Matsumine H, Asakawa S, Kitada T, Yoshino H, et al. (1998) Point mutations (Thr240Arg and Gln311Stop) [correction of Thr240Arg and Ala311Stop] in the Parkin gene. Biochem Biophys Res Commun 249: 754–758.
3. Lucking CB, Durr A, Bonifati V, Vaughan J, De Michele G, et al. (2000) Association between early-onset Parkinson's disease and mutations in the parkin gene. N Engl J Med 342: 1560–1567.
4. Gasser T (2009) Molecular pathogenesis of Parkinson disease: insights from genetic studies. Expert Rev Mol Med 11: e22.
5. Cookson MR, Bandmann O (2010) Parkinson's disease: insights from pathways. Hum Mol Genet 19: R21–27.
6. Benner EJ, Banerjee R, Reynolds AD, Sherman S, Pisarev VM, et al. (2008) Nitrated alpha-synuclein immunity accelerates degeneration of nigral dopaminergic neurons. PLoS One 3: e1376.
7. Kuhn DM, Francescutti-Verbeem DM, Thomas DM (2006) Dopamine quinones activate microglia and induce a neurotoxic gene expression profile: relationship to methamphetamine-induced nerve ending damage. Ann N Y Acad Sci 1074: 31–41.
8. Reynolds AD, Kadiu I, Garg SK, Glanzer JG, Nordgren T, et al. (2008) Nitrated alpha-synuclein and microglial neuroregulatory activities. J Neuroimmune Pharmacol 3: 59–74.
9. Goedert M (2001) Alpha-synuclein and neurodegenerative diseases. Nat Rev Neurosci 2: 492–501.
10. Spillantini MG, Crowther RA, Jakes R, Hasegawa M, Goedert M (1998) alpha-Synuclein in filamentous inclusions of Lewy bodies from Parkinson's disease and dementia with lewy bodies. Proc Natl Acad Sci U S A 95: 6469–6473.
11. Spillantini MG, Schmidt ML, Lee VM, Trojanowski JQ, Jakes R, et al. (1997) Alpha-synuclein in Lewy bodies. Nature 388: 839–840.
12. Mizuno Y, Hattori N, Mori H, Suzuki T, Tanaka K (2001) Parkin and Parkinson's disease. Curr Opin Neurol 14: 477–482.
13. Farrer M, Chan P, Chen R, Tan L, Lincoln S, et al. (2001) Lewy bodies and parkinsonism in families with parkin mutations. Ann Neurol 50: 293–300.
14. Pramstaller PP, Schlossmacher MG, Jacques TS, Scaravilli F, Eskelson C, et al. (2005) Lewy body Parkinson's disease in a large pedigree with 77 Parkin mutation carriers. Ann Neurol 58: 411–422.
15. Sasaki S, Shirata A, Yamane K, Iwata M (2004) Parkin-positive autosomal recessive juvenile Parkinsonism with alpha-synuclein-positive inclusions. Neurology 63: 678–682.
16. Winslow AR, Rubinsztein DC (2011) The Parkinson disease protein alpha-synuclein inhibits autophagy. Autophagy 7: 429–431.
17. Winslow AR, Chen CW, Corrochano S, Acevedo-Arozena A, Gordon DE, et al. (2010) alpha-Synuclein impairs macroautophagy: implications for Parkinson's disease. J Cell Biol 190: 1023–1037.
18. Imai Y, Soda M, Takahashi R (2000) Parkin suppresses unfolded protein stress-induced cell death through its E3 ubiquitin-protein ligase activity. J Biol Chem 275: 35661–35664.
19. Shimura H, Hattori N, Kubo S, Mizuno Y, Asakawa S, et al. (2000) Familial Parkinson disease gene product, parkin, is a ubiquitin-protein ligase. Nat Genet 25: 302–305.
20. Zhang Y, Gao J, Chung KK, Huang H, Dawson VL, et al. (2000) Parkin functions as an E2-dependent ubiquitin- protein ligase and promotes the degradation of the synaptic vesicle-associated protein, CDCrel-1. Proc Natl Acad Sci U S A 97: 13354–13359.
21. Narendra D, Tanaka A, Suen DF, Youle RJ (2008) Parkin is recruited selectively to impaired mitochondria and promotes their autophagy. J Cell Biol 183: 795–803.
22. Olzmann JA, Chin LS (2008) Parkin-mediated K63-linked polyubiquitination: a signal for targeting misfolded proteins to the aggresome-autophagy pathway. Autophagy 4: 85–87.
23. Vincow ES, Merrihew G, Thomas RE, Shulman NJ, Beyer RP, et al. (2013) The PINK1-Parkin pathway promotes both mitophagy and selective respiratory chain turnover in vivo. Proc Natl Acad Sci U S A 110(16): 6400–6405.
24. Lonskaya I, Hebron ML, Algarzae NK, Desforges N, Moussa CE (2012) Decreased parkin solubility is associated with impairment of autophagy in the nigrostriatum of sporadic Parkinson's disease. Neuroscience 232C: 90.
25. Lonskaya I, Shekoyan AR, Hebron ML, Desforges N, Algarzae NK, et al. (2013) Diminished parkin solubility and co-localization with intraneuronal amyloid-beta are associated with autophagic defects in Alzheimer's disease. J Alzheimers Dis 33: 231–247.
26. Ko HS, Lee Y, Shin JH, Karuppagounder SS, Gadad BS, et al. (2010) Phosphorylation by the c-Abl protein tyrosine kinase inhibits parkin's ubiquitination and protective function. Proc Natl Acad Sci U S A 107: 16691–16696.
27. Lonskaya I, Shekoyan AR, Hebron ML, Desforges N, Algarzae NK, et al. (2012) Diminished Parkin Solubility and Co-Localization with Intraneuronal Amyloid-beta are Associated with Autophagic Defects in Alzheimer's Disease. J Alzheimers Dis.
28. Rodriguez-Navarro JA, Gomez A, Rodal I, Perucho J, Martinez A, et al. (2008) Parkin deletion causes cerebral and systemic amyloidosis in human mutated tau over-expressing mice. Hum Mol Genet 17: 3128–3143.
29. Dawson TM, Dawson VL (2010) The role of parkin in familial and sporadic Parkinson's disease. Mov Disord 25 Suppl 1: S32–39.
30. Hebron ML, Lonskaya I, Moussa CE (2013) Nilotinib reverses loss of dopamine neurons and improves motor behavior via autophagic degradation of alpha-synuclein in Parkinson's disease models. Hum Mol Genet 22: 3315–3328.
31. Imam SZ, Zhou Q, Yamamoto A, Valente AJ, Ali SF, et al. (2011) Novel regulation of parkin function through c-Abl-mediated tyrosine phosphorylation: implications for Parkinson's disease. J Neurosci 31: 157–163.

32. Kantarjian HM, Giles F, Gattermann N, Bhalla K, Alimena G, et al. (2007) Nilotinib (formerly AMN107), a highly selective BCR-ABL tyrosine kinase inhibitor, is effective in patients with Philadelphia chromosome-positive chronic myelogenous leukemia in chronic phase following imatinib resistance and intolerance. Blood 110: 3540−3546.
33. de Lavallade H, Apperley JF, Khorashad JS, Milojkovic D, Reid AG, et al. (2008) Imatinib for newly diagnosed patients with chronic myeloid leukemia: incidence of sustained responses in an intention-to-treat analysis. J Clin Oncol 26: 3358−3363.
34. Lonskaya I, Hebron ML, Desforges NM, Franjie A, Moussa CE (2013) Tyrosine kinase inhibition increases functional parkin-Beclin-1 interaction and enhances amyloid clearance and cognitive performance. EMBO Mol Med 5(8): 1247−1262.
35. Burns MP, Zhang L, Rebeck GW, Querfurth HW, Moussa CE (2009) Parkin promotes intracellular Abeta1-42 clearance. Hum Mol Genet 18: 3206−3216.
36. Herman AM, Moussa CE (2011) The ubiquitin ligase parkin modulates the execution of autophagy. Autophagy 7: 919−921.
37. Khandelwal PJ, Dumanis SB, Feng LR, Maguire-Zeiss K, Rebeck G, et al. (2010) Parkinson-related parkin reduces alpha-Synuclein phosphorylation in a gene transfer model. Mol Neurodegener 5: 47.
38. Hebron ML, Lonskaya I, Sharpe K, Weerasinghe PP, Algarzae NK, et al. (2013) Parkin Ubiquitinates Tar-DNA Binding Protein-43 (TDP-43) and Promotes Its Cytosolic Accumulation via Interaction with Histone Deacetylase 6 (HDAC6). J Biol Chem 288: 4103−4115.
39. Lonskaya I, Hebron ML, Desforges NM, Franjie A, Moussa CE (2013) Tyrosine kinase inhibition increases functional parkin-Beclin-1 interaction and enhances amyloid clearance and cognitive performance. EMBO Mol Med.
40. Goldberg MS, Fleming SM, Palacino JJ, Cepeda C, Lam HA, et al. (2003) Parkin-deficient mice exhibit nigrostriatal deficits but not loss of dopaminergic neurons. J Biol Chem 278: 43628−43635.
41. Giasson BI, Duda JE, Quinn SM, Zhang B, Trojanowski JQ, et al. (2002) Neuronal alpha-synucleinopathy with severe movement disorder in mice expressing A53T human alpha-synuclein. Neuron 34: 521−533.
42. Kitada T, Pisani A, Karouani M, Haburcak M, Martella G, et al. (2009) Impaired dopamine release and synaptic plasticity in the striatum of parkin−/− mice. J Neurochem 110: 613−621.
43. Riley BE, Lougheed JC, Callaway K, Velasquez M, Brecht E, et al. (2013) Structure and function of Parkin E3 ubiquitin ligase reveals aspects of RING and HECT ligases. Nat Commun 4: 1982.
44. Lazarou M, Narendra DP, Jin SM, Tekle E, Banerjee S, et al. (2013) PINK1 drives Parkin self-association and HECT-like E3 activity upstream of mitochondrial binding. J Cell Biol 200: 163−172.
45. Wenzel DM, Lissounov A, Brzovic PS, Klevit RE (2011) UBCH7 reactivity profile reveals parkin and HHARI to be RING/HECT hybrids. Nature 474: 105−108.
46. Iguchi M, Kujuro Y, Okatsu K, Koyano F, Kosako H, et al. (2013) Parkin-catalyzed ubiquitin-ester transfer is triggered by PINK1-dependent phosphorylation. J Biol Chem 288: 22019−22032.
47. Spratt DE, Martinez-Torres RJ, Noh YJ, Mercier P, Manczyk N, et al. (2013) A molecular explanation for the recessive nature of parkin-linked Parkinson's disease. Nat Commun 4: 1983.
48. Zheng X, Hunter T (2013) Parkin mitochondrial translocation is achieved through a novel catalytic activity coupled mechanism. Cell Res 23: 886−897.
49. Matsuda N, Sato S, Shiba K, Okatsu K, Saisho K, et al. (2010) PINK1 stabilized by mitochondrial depolarization recruits Parkin to damaged mitochondria and activates latent Parkin for mitophagy. J Cell Biol 189: 211−221.
50. Wauer T, Komander D (2013) Structure of the human Parkin ligase domain in an autoinhibited state. EMBO J 32(15): 2099−2112.
51. Trempe JF, Sauve V, Grenier K, Seirafi M, Tang MY, et al. (2013) Structure of parkin reveals mechanisms for ubiquitin ligase activation. Science 340: 1451−1455.
52. Chaugule VK, Burchell L, Barber KR, Sidhu A, Leslie SJ, et al. (2011) Autoregulation of Parkin activity through its ubiquitin-like domain. EMBO J 30: 2853−2867.
53. Khandelwal PJ, Herman AM, Hoe HS, Rebeck GW, Moussa CE (2011) Parkin mediates beclin-dependent autophagic clearance of defective mitochondria and ubiquitinated Abeta in AD models. Hum Mol Genet 20: 2091−2102.
54. Rosen KM, Moussa CE, Lee HK, Kumar P, Kitada T, et al. (2010) Parkin reverses intracellular beta-amyloid accumulation and its negative effects on proteasome function. J Neurosci Res 88: 167−178.
55. Lagier-Tourenne C, Polymenidou M, Hutt KR, Vu AQ, Baughn M, et al. (2012) Divergent roles of ALS-linked proteins FUS/TLS and TDP-43 intersect in processing long pre-mRNAs. Nat Neurosci 15: 1488−1497.
56. Kim NC, Tresse E, Kolaitis RM, Molliex A, Thomas RE, et al. (2013) VCP Is Essential for Mitochondrial Quality Control by PINK1/Parkin and this Function Is Impaired by VCP Mutations. Neuron 78(1): 65−80.
57. Henn IH, Gostner JM, Lackner P, Tatzelt J, Winklhofer KF (2005) Pathogenic mutations inactivate parkin by distinct mechanisms. J Neurochem 92: 114−122.
58. Sriram SR, Li X, Ko HS, Chung KK, Wong E, et al. (2005) Familial-associated mutations differentially disrupt the solubility, localization, binding and ubiquitination properties of parkin. Hum Mol Genet 14: 2571−2586.
59. Hampe C, Ardila-Osorio H, Fournier M, Brice A, Corti O (2006) Biochemical analysis of Parkinson's disease-causing variants of Parkin, an E3 ubiquitin-protein ligase with monoubiquitylation capacity. Hum Mol Genet 15: 2059−2075.
60. Mollenhauer B, Trautmann E, Otte B, Ng J, Spreer A, et al. (2012) alpha-Synuclein in human cerebrospinal fluid is principally derived from neurons of the central nervous system. J Neural Transm 119: 739−746.
61. Jiang H, Ren Y, Yuen EY, Zhong P, Ghaedi M, et al. (2012) Parkin controls dopamine utilization in human midbrain dopaminergic neurons derived from induced pluripotent stem cells. Nat Commun 3: 668.